DEVELOPMENTAL DYNAMICS 245:614–626, 2016
DOI: 10.1002/DVDY.24399

Transcriptome of the Inner Circular Smooth Muscle of the Developing Mouse Intestine: Evidence for Regulation of Visceral Smooth Muscle Genes by the Hedgehog Target Gene, *cJun*

Katherine Gurdziel,[1,2] Kyle R. Vogt,[1] Katherine D. Walton,[1] Gary K. Schneider,[1] and Deborah L. Gumucio[1]*

[1]Department of Cell and Developmental Biology, University of Michigan, Ann Arbor, MI 48109
[2]Department of Computational Medicine and Bioinformatics, University of Michigan, Ann Arbor, MI 48109

Background: Digestion is facilitated by coordinated contractions of the intestinal muscularis externa, a bilayered smooth muscle structure that is composed of inner circular muscles (ICM) and outer longitudinal muscles (OLM). We performed transcriptome analysis of intestinal mesenchyme tissue at E14.5, when the ICM, but not the OLM, is present, to investigate the transcriptional program of the ICM. Results: We identified 3967 genes enriched in E14.5 intestinal mesenchyme. The gene expression profiles were clustered and annotated to known muscle genes, identifying a muscle-enriched subcluster. Using publically available in situ data, 127 genes were verified as expressed in ICM. Examination of the promoter and regulatory regions for these co-expressed genes revealed enrichment for cJUN transcription factor binding sites, and cJUN protein was enriched in ICM. cJUN ChIP-seq, performed at E14.5, revealed that cJUN regulatory regions contain characteristics of muscle enhancers. Finally, we show that *cJun* is a target of Hedgehog (Hh), a signaling pathway known to be important in smooth muscle development, and identify a *cJun* genomic enhancer that is responsive to Hh. Conclusions: This work provides the first transcriptional catalog for the developing ICM and suggests that *cJun* regulates gene expression in the ICM downstream of Hh signaling. *Developmental Dynamics 245:614–626, 2016*. © 2016 Wiley Periodicals, Inc.

Key words: intestinal development; visceral smooth muscle; *cJun*; Hedgehog signaling; enhancers

Submitted 20 November 2015; First Decision 29 January 2016; Accepted 16 February 2016; Published online 1 March 2016

Introduction

Smooth muscle is a critical component for the function of many organs, including respiratory (Tollet et al., 2001; Goyal and Chaudhury, 2008), urogenital (Baker and Gomez, 1998; DiSandro et al., 1998), and gastrointestinal tissues. The adult intestine contains several populations of intestinal smooth muscle (ISM), located in different regions of the tube. A thin muscularis mucosa lies just beneath the epithelium, while the muscularis externa (ME) forms the outside of the tube, surrounding the mucosa and submucosa. The bilayered ME contains an inner circular muscle (ICM) and outer longitudinal muscle (OLM), with enteric nerves nestled between these layers (Gabella, 1985; Thomason et al., 2012).

The smooth muscle populations of the ME are of particular clinical interest because of their critical role in gut motility (Bitar, 2003). Alterations to muscle contractility are seen in irritable bowel syndrome (Whorwell et al., 1986; Van der Vliet et al., 1992; Abrams et al., 2012) and during gut inflammation (Ohama et al., 2007). Some forms of chronic intestinal pseudo-obstruction are also rooted in ISM pathology (visceral myopathy) (Antonucci et al., 2008). Both familial (Anuras et al., 1981; Sipponen et al., 2009) and sporadic (Montalvo et al., 2004) cases of visceral myopathy have been reported, and a few susceptibility loci have been identified, including DNA POLG (chromosome (Chr) 21) (Vissing et al., 2002; Van Goethem et al., 2003; Giordano et al., 2009) and ACTG2 (Ch 2) (Lehtonen et al., 2012; Holla et al., 2014; Thorson et al., 2014; Wangler et al., 2014). Interestingly, the various ISM layers can be differently affected. Pathological changes specific to the muscularis mucosae (Alstead et al., 1988) or to the OLM (Anuras et al., 1983) have been reported, and loss of alpha-smooth muscle actin (αSMA) expression has been noted specifically in the ICM (Smith et al., 1992; Donnell et al., 2008).

In addition to their distinct patterns of pathology, the layers of ISM develop in different time windows. The ICM is the first layer to appear; it is well developed by embryonic day 14 (E14). The OLM becomes clearly organized by E16 (Kedinger et al., 1990; Thomason et al., 2012). Development of villus smooth muscle occurs at approximately E18, while the sub-epithelial muscularis

Additional supporting information may be found in the online version of this article.

*Correspondence to: Deborah L. Gumucio, 109 Zina Pitcher Place, Ann Arbor, MI 48109; 734-647-0172. E-mail: dgumucio@umich.edu

Article is online at: http://onlinelibrary.wiley.com/doi/10.1002/dvdy.24399/abstract

TABLE 1. GSEA Muscle Gene Sets Enriched in E14.5 Intestinal Mesenchyme Tissue

Gene Set	Genes found	Set size	Enrichment score	NOM *p*-value
KEGG_VASCULAR_SMOOTH_MUSCLE_CONTRACTION	37	115	0.378421	0
KEGG_CARDIAC_MUSCLE_CONTRACTION	25	81	0.374815	3.4x10-2
REACTOME_MUSCLE_CONTRACTION	18	48	0.321722	2.1x10-2
KAYO_CALORIE_RESTRICTION_MUSCLE_DN	15	89	0.297956	3.3 x10-2
KAYO_AGING_MUSCLE_UP	59	206	0.249085	1.1 x10-2
ROME_INSULIN_TARGETS_IN_MUSCLE_DN	34	246	0.204829	4.8 x10-2
KAYO_CALORIE_RESTRICTION_MUSCLE_UP	30	95	0.201314	4.8 x10-2
MUSCLE_DEVELOPMENT	35	93	0.149875	4.6 x10-2

mucosa matures after birth (Kolterud et al., 2009; Zacharias et al., 2011).

Despite their critical importance to gut homeostasis, little is known about the molecular characteristics or gene regulatory programs of any of the ISM layers. In this study, we report the first transcriptome profile for the embryonic intestinal ICM. The early development of the ICM allowed us the opportunity to restrict the analysis to that layer. Using clustering analysis of RNA-seq data in combination with publically available in situ expression data for the E14.5 mouse (Visel et al., 2004; Diez-Roux et al., 2011), we identified a subcluster of more than 100 genes with confirmed expression in the ICM, and analyzed the promoters of co-clustered genes to identify transcription factors that might be involved in the regulation of these ISM genes. Among these enriched transcription factors was cJUN; antibody staining of intestinal sections confirmed that cJUN protein is strongly expressed in ICM. Further ChIP-seq studies identified 2741 potential cJUN regulatory regions that are also expressed in ICM. Our data suggest a previously undocumented role for cJUN in the regulation of the ICM transcriptional program.

We also further explored the regulatory relationship between cJUN and Hedgehog (Hh) signaling with respect to ICM gene regulation. Hh has been previously shown to be important in activating gene expression in smooth muscle of several tissues, including the bladder (Shiroyanagi et al., 2007; Liu et al., 2010; Tasian et al., 2010), intestine (Sukegawa et al., 2000; Kolterud et al., 2009; Zacharias et al., 2011; Huang et al., 2013), and ureter (Yu et al., 2002; Caubit et al., 2008). Here, we document that cJUN is a Hh target and identify an enhancer that mediates Hh-dependent cJUN induction.

Results and Discussion

Identification of Intestinal Visceral Smooth Muscle Genes

We began this analysis by identifying genes that are enriched in the mesenchymal layer of the E14.5 intestine. To do this, we separated epithelial and mesenchymal tissue populations from WT mouse intestines at E14.5 and collected RNA from each layer for high-throughput sequencing (see Methods). The two transcriptomes were compared to identify genes that were differentially expressed between the intestinal mesenchyme (which contains muscle) and the intestinal epithelial tissue (which is devoid of muscle). This analysis identified 3967 (adjusted *P* value $\leq$ 0.05) genes that were at least twofold enriched in the mesenchyme tissue (Supp. Table S1, which is available online).

To begin to identify potential smooth muscle genes within this enriched set, we used Gene Set Enrichment Analysis (GSEA) (Subramanian et al., 2005). Although its Molecular Signatures Database contained no sets of enriched muscle genes derived from ISM tissue, we reasoned that due to its contractile nature, some smooth muscle genes might overlap with genes identified in vascular, cardiac, and skeletal muscle. Indeed, overlap between gene expression and regulatory programs in muscle subtypes has been previously observed (Li et al., 1996). Comparing those muscle gene sets to our 3967 mesenchymally enriched genes identified 253 putative ISM genes (enriched muscle gene sets, *P* value $\leq$ 0.05, are listed in Table 1). Using publically available in situ images (Visel et al., 2004; Diez-Roux et al., 2011), we next examined the expression pattern of each of these 253 genes in E14.5 mouse intestine. This analysis confirmed 33 genes that exhibited clear expression in the area of the ICM (Fig. 1A).

To further expand this ISM data set, we hierarchically clustered genes that are up-regulated in the mesenchyme (Eisen et al., 1998). Since many of the 33 identified genes were structural genes associated with contractility, we expected that they might be expressed at similar levels within the mesenchyme and that other, similarly expressed genes might also cluster with these genes. Indeed, Figure 1B shows that when the expression profiles of 9490 mesenchymally expressed genes are clustered, all 33 genes with verified expression in the ICM domain (annotated with black tick marks) fall into the same subcluster of 1312 genes. Other genes within this same subcluster, with an average expression value $>$ 500, were then examined for localized expression within the ICM (Visel et al., 2004; Diez-Roux et al., 2011). This comparison identified an additional 94 genes that are expressed in the ICM (Fig. 1C).

Among the genes that are expressed in the ICM, several (e.g., *Actc1*, *Lmod1*, *Myom1*, *Tnnt2*) were associated with other muscle types (Gunning et al., 1984; Vinkemeier et al., 1993; Townsend et al., 1994; Zhang et al., 1996). Others are apparently unique to smooth muscle (e.g., *Cav1*, *Cnn1*, *Myl9*, *Smtn*, *Tagln*) (Lees-Miller et al., 1987; Kumar et al., 1989; Strasser et al., 1993; van der Loop et al., 1996; Austin et al., 2012). Several expected muscle regulatory factors (e.g., *Mef2C*, *Myocd*, and *SRF*) are present in the expression profile and are expressed in the ICM according to the in situ database, GenePaint.org (Miano, 2003; Wang et al., 2003; Creemers et al., 2006). Additionally, several components or

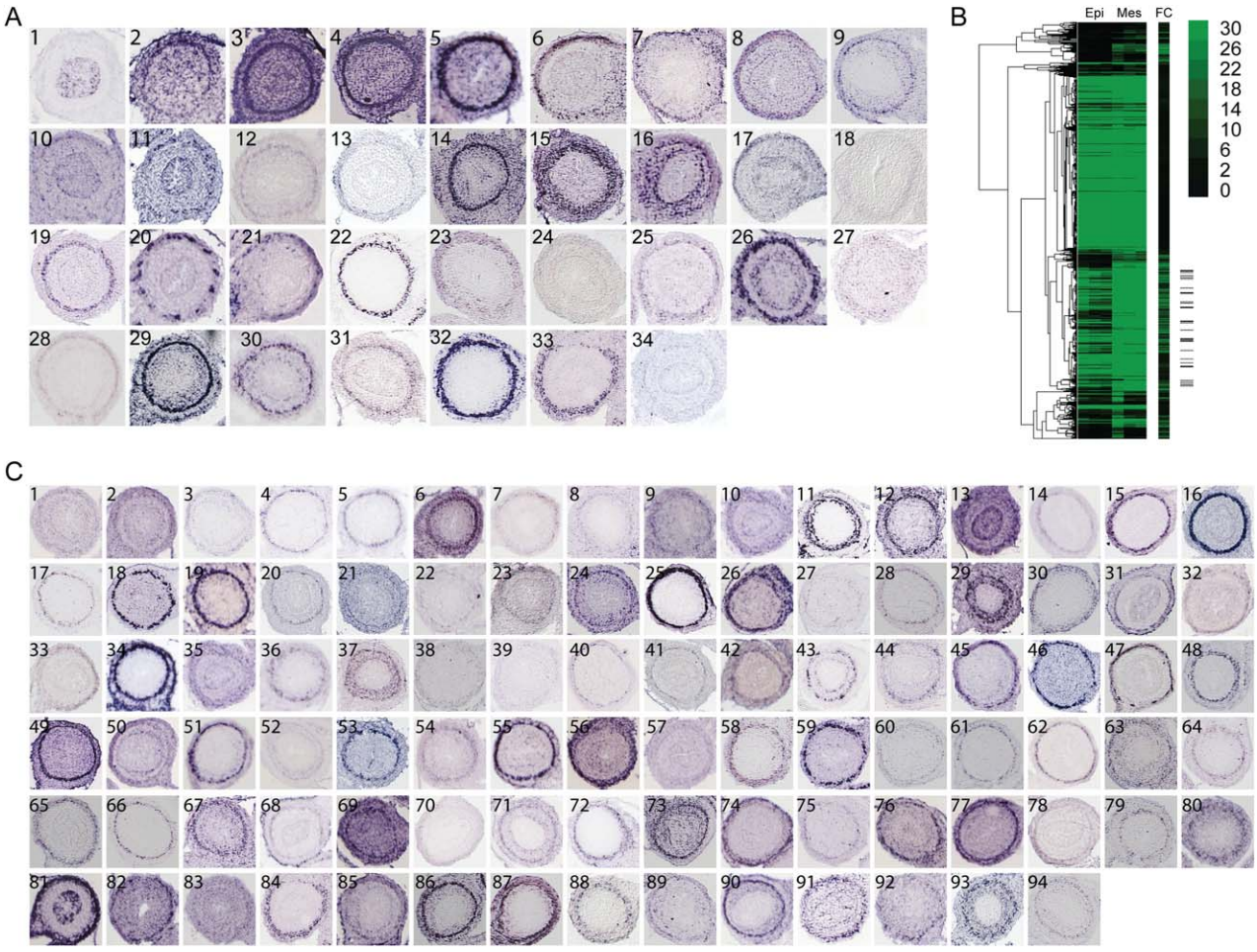

Fig. 1. Identification of intestinal visceral smooth muscle genes. **(A)** RNA in situ localization images of (A1) epithelial marker Cdx1 [EH4673] and (A2–A34) GSEA identified prospective intestinal smooth muscle (ISM) genes with ICM localization at E14.5. Intestinal cross sections are from GenePaint.org (Set ID in brackets). Panels are (2) ACTC1 [DC37], (3) ACTA2 [EH2333], (4) ACTG2 [ES688], (5) ADCY5 [MH851], (6) ATP1A2 [EN427], (7) BOC [EB1453], (8) CACNA1H [ES1420], (9) CALD1 [EG423], (10) CCL2 [EH401], (11) CNP1 [EH672], (12) DDR2 [EH3223], (13) DES [EH1766], (14) FLNA [EN2546], (15) FN1 [EN386], (16) FOXF2 [MH3070], (17) FXYD2 [EH804], (18) GLI3 [MH1026], (19) LMOD1 [EH4061], (20) MAPT [EH1455], (21) MEF2C [MH765], (22) MYL9 [EB2526], (23) NCAM1 [ES2731], (24) PLAU [MH1483], (25) PLCB4 [EH4161], (26) RBP1 [EH1743], (27) SALL2 [EH4737], (28) SLC8A1 [MH1892], (29) SMTN [EH1228], (30) SORBS1 [EH2043], (31) SVIL [EN1436], (32) TAGLN [EB415], (33) TGFBR2 [EB1113], and (34) TNNT2 [EH505]. **(B)** Hierarchically clustered expression data containing three replicates of epithelial (Epi, first three columns) and mesenchyme (Mes, next three columns) read counts for genes up-regulated in mesenchyme. Fold change (FC) is depicted in the additional column. The locations of the confirmed smooth muscle genes (A2–A34) are denoted on the right with black tick marks. **(C)** RNA in situ analysis of 94 other genes within the subcluster of confirmed GSEA enriched genes showing ICM localization. (1) ABI2 [EH4750], (2) ACOT7 [EH3555], (3) ADAM19 [EB509], (4) ADAMTS8 [EB1785], (5) ADCY5 [MH851], (6) AKAP2 [EH3708], (7) AKAP6 [EH3709], (8) AKAP12 [EB1789], (9) AKT3 [EH2186], (10) ATP2B4 [EG2318], (11) CAV1 [EG91], (12) CASQ1 [EN103], (13) CBX6 [EH1869], (14) CCKAR [EH3710], (15) CHRM2 [EH2853], (16) CNN1 [EH1511], (17) CRISPLD2 [ES1352], (18) CRMP1 [ES1162], (19) CTTNBP2 [EH1103], (20) EFS [EH2735], (21) CUEDC1 [EH1301], (22) DDR2 [EH3223], (23) DUSP10 [MH1605], (24) CSPR1 [HD13], (25) ENC1 [MH749], (26) FNBP1 [ES598], (27) FBXO32 [ES255], (28) FOXP2 [EG742], (29) EMILIN3 [EB1359], (30) FOXF1 [MH3518], (31) GDNF [EH574], (32) GAB2 [EN1340], (33) FREM2 [EN2329], (34) FZD3 [MH732], (35) GAS1 [MH360], (36) GEM [EH1664], (37) GNAQ [EN2590], (38) GPR20 [EH2873], (39) GLI1 [EN1215], (40) HAND1 [MH519], (41) GREM2 [EH1239], (42) GREM1 [EB63], (43) HOXB5 [EH612], (44) HHIP [EB1363], (45) HOXA5 [EN692], (46) HOXD3 [EN1290], (47) HOXB4 [MH3073], (48) ID4 [EN2437], (49) ITIH5 [EH3960], (50) ITGA9 [EH3560], (51) ITGA5 [EH3234], (52) KCNIP1 [EH1584], (53) LEBREL1 [EH4020], (54) IGFBP2 [ES388], (55) LRGI1 [MH431], (56) MYADM [EG746], (57) MTAP1B [ES1557], (58) MRVI1 [ES819], (59) LTBP1 [EH4243], (60) MAPK8IP1 [EH3404], (61) NEXN [ES414], (62) MYOCD [EN2445], (63) NCAM1 [ES2731], (64) MYOM1 [DC35], (65) NCALD [EG960], (66) NELL2 [EG1866], (67) NRBP2 [EH2160], (68) PSD [EB1667], (69) NPNT [MH2326], (70) PCDH7 [EB2060], (71) NKD1 [EB1514], (72) PKRG1 [EB1942], (73) PTN [EH3730], (74) PTMS [EG1747], (75) RGMA [EH2791], (76) RSPO3 [EN1484], (77) RARB [EH1089], (78) PYGL [MH3193], (79) SOX12 [MH3020], (80) SMOC2 [EH2269], (81) TGFB2 [EB1113], (82) SLC24A3 [MH3376], (83) SLC22A17 [MH2066], (84) SOX4 [MH3053], (85) TGFB1I1 [EG2803], (86) TGFB3 [EH2000], (87) TSPAN9 [EH2385], (88) THBS4 [MH1698], (89) THBS2 [ES844], (90) TMEM47 [EH2893], (91) TSHZ1 [EB2573], (92) TULP4 [MY240], (93) ZYX [EG1608], and (94) WWTR1 [EH904].

known targets of the Hh signaling pathway (e.g., *Boc, Gli1, Gli3, Hhip, Mef2C, Myocd*), some of which are known to be enriched in ISM (Kolterud et al., 2009), are present in the list.

These 127 genes are clearly not a comprehensive catalog of ICM gene expression. The analysis is based on one developmental time period (E14.5), and the study was purposefully initiated using genes that are mesenchymally enriched at this time and expressed at medium to high levels. For example, *Arid5b*, a regulator of smooth muscle differentiation (Watanabe et al., 2002), is not differentially expressed between epithelial and mesenchyme

tissue (Teillet et al., 1998), and the SM-associated genes, *Il1b* and *Mitf*, are both expressed in the mesenchyme but at low levels (Chen et al., 2006; Chi et al., 2007). We also excluded genes that are not expressed in the ICM at E14.5. For example, *Pbx1*, a transcription factor associated with myogenic programs (Berkes et al., 2004), is mesenchymally enriched in our data set but is not present in the ICM at this time point (GenePaint ID: ES1284).

Identification of Transcriptional Regulators of Intestinal Visceral Smooth Muscle Genes

To begin to identify transcription factors that might be responsible for coordinating smooth muscle gene expression, we next used DiRE (Gotea and Ovcharenko, 2008) to analyze the promoter regions of the 1312 genes in the muscle gene subcluster. The top 10 transcription factors enriched in these gene promoters included several known to be involved in regulatory programs in skeletal muscle or in vascular smooth muscle, including RP58, NF1, TAL1, NOTCH1, PAX4, cJUN, HOXA9, and MEIS1 (Fig. 2A) (Kami et al., 1995; Tao et al., 1998; Knoepfler et al., 1999; Daury et al., 2001; Ema et al., 2003; Di Padova et al., 2007; Yokoyama et al., 2009; Kossler et al., 2011; Raines et al., 2013; Mourikis and Tajbakhsh, 2014; Summers et al., 2015). To narrow this putative regulator list to those potentially relevant to ICM regulation, we again turned to the in situ patterns. Of the top 10 enriched transcription factors, cJUN is unique in that it is expressed robustly in the ICM region at E14.5 (Fig. 2K). Thus, we further examined the role of cJUN in ISM expression.

To confirm cJUN expression in ICM, we examined whether this protein co-localizes with the smooth muscle marker αSMA and with GLI1, a target of Hh signaling that is required for ISM development and maintenance (Ramalho-Santos et al., 2000; Sukegawa et al., 2000; Madison et al., 2005; Kolterud et al., 2009; Zacharias et al., 2011). Intestines from *Gli1*$^{eGFP/+}$ mice were immunostained with anti-cJUN, anti-αSMA, and anti-eGFP (*Gli1*) at key time points during ISM development (E12.5, E14.5, E16.5, and E18.5). At E12.5, prior to formation of the ICM, αSMA staining marks subepithelial mesenchymal cells. Neither GLI1 nor cJUN localize with cells staining positive for αSMA at this stage (Fig. 3A–D). However, GLI1 and cJUN co-localize in a different subset of mesenchymal cells of unknown type (Fig. 3R,T). By E14.5, when the ICM is clearly formed, cJUN co-localizes entirely with αSMA (Fig. 3G,H). GLI1 (eGFP) expression is most robust in the inner boundary of the ICM (Fig. 3F), as shown previously (Kolterud et al., 2009). At E16.5, cJUN and αSMA mark both the ICM and the newly established outer OLM layer (Fig. 3K,L). GLI1 remains most strongly expressed in the ICM (Fig. 3J). At E18.5, αSMA marks the cells in the inner circular, outer longitudinal, and villus core muscles (Fig. 3W). Neither GLI1 nor cJUN is expressed in the villus core muscle prior to birth; however, both are still expressed within the ICM (Fig. 3NP). In addition, these two markers stain a population of vascular smooth muscle cells in the submucosal vascular plexus (Fig. 3V,X).

Identification of cJUN Binding Locations in E14.5 Intestines

Taken together, these data suggest that cJUN may be a regulator of ISM genes: It is enriched in the promoters of mesenchymally enriched genes, and it exclusively marks the ICM region at E14.5. To investigate this further, we used ChIP-seq to identify cJUN binding sites. Intestines from E14.5 C57BL/6J fetuses were harvested and grown in culture under conditions identical to the collection of the epithelial and mesenchyme profiles, except that the tissue separation was not done. ChIP was performed on whole intestines with cJUN antibody, and the resulting libraries were sequenced. In total, 21.1 million cJUN-immunoprecipitated and 23.5 million input 50-bp short reads were generated. Using a P value threshold of < 0.05, 2741 sequence peaks were identified by comparing read enrichment from cJUN-immunoprecipitated DNA to input control.

The sequence peaks (see Supp. Table S2, which is available online) were annotated to the nearest gene by measuring the distance between the coordinates of the center of the peak and the transcriptional start sites (TSS) of neighboring genes. Location of the peak was then categorized as 5′ distal, within 2Kbp of the promoter, within the gene, 3′ proximal, 3′ distal, or within a gene desert (> 100 Kbp from the TSS or transcription end site [TES]). All peaks that mapped within genes were intronic. Since the majority of peaks were found in gene deserts outside of the immediate vicinity of a gene (Fig. 4A), we examined the conservation of these regions (Fig. 4B). This analysis demonstrated that conservation was highest in the central peak regions, suggesting that these regions are functionally important (Fig. 4B).

Motif analysis of the cJUN peaks revealed enrichment of several muscle-associated transcription factors (Fig. 4C). Of particular interest here is the enrichment for SRF, which, with its cofactor, myocardin, is a master regulator of smooth muscle gene expression (Wang et al., 2003; Wang et al., 2004). Enrichment of SRF sites with cJUN sites further supports the idea that these regulatory regions are active in ISM. Other enriched factors of the SOX, FOXO, HOX, TEAD, and EGR families were also noted. Members of all these families have been implicated in the regulation of cardiac muscle, skeletal muscle and/or vascular smooth muscle (Wang et al., 2001; Schmidt et al., 2003; Wada et al., 2003; Lee et al., 2004; Liu et al., 2005; Meeson et al., 2007; Papanicolaou et al., 2008; Qiu et al., 2011; Benhaddou et al., 2012; Fan et al., 2013; Wang et al., 2013; Liu et al., 2014; Sanchez et al., 2014), though none have been previously characterized in visceral smooth muscle.

To functionally verify enhancer activity, four cJUN peaks were screened for responsiveness in a muscle cell culture assay. The putative regulatory regions were cloned upstream of a minimal promoter that drives luciferase expression and transiently transfected into C2C12 cells along with either a plasmid encoding full-length cJUN or a dominant negative version of cJUN (see Methods). For the four regulatory regions tested, all were up-regulated when co-expressed with cJUN. In all cases, co-transfection with the dominant negative cJUN construct diminished luciferase expression (Fig. 5A).

Relationship Between Hh Signaling and cJUN Transcription in ISM Development

Previous studies suggested the possibility that cJUN and GLI1 might act together to co-regulate genes, since the two factors bind together at the human cJUN promoter (Laner-Plamberger et al., 2009; Amable et al., 2014). The Hh signaling pathway is an established regulator of the development of both the ME and the villus smooth muscle populations (Sukegawa et al., 2000; Yu et al., 2002; Shiroyanagi et al., 2007; Caubit et al., 2008; Kolterud

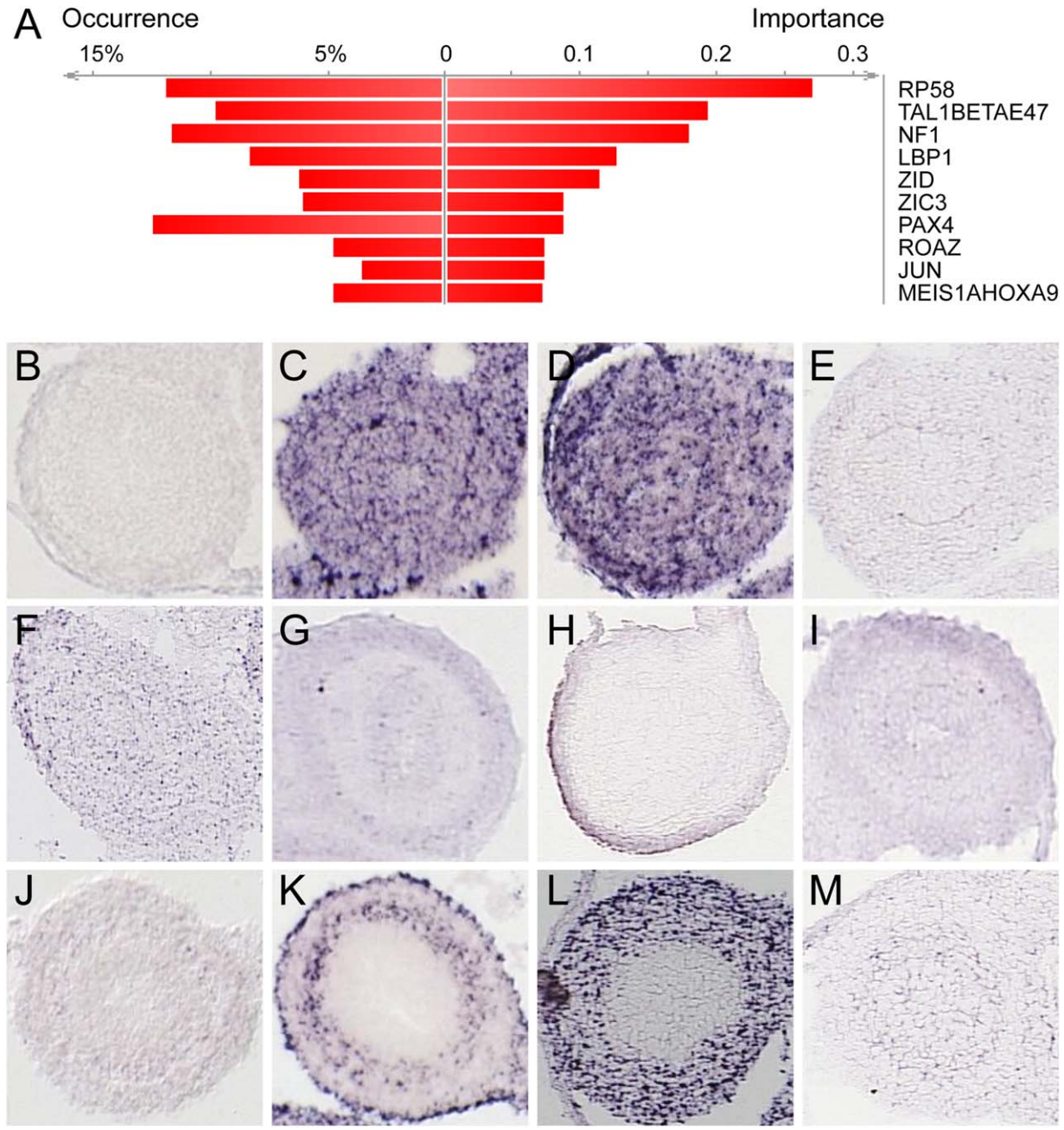

Fig. 2. cJUN is enriched in the promoters of up-regulated mesenchyme genes and is expressed in intestinal inner circular muscles (ICM) at E14.5. **(A)** The top 10 promoter-enriched transcription factors (TF) identified by DiRE include known muscle regulators RP58, NF1, ZIC3, and the MEIS1/HOXA9 complex. Occurrence indicates the percentage of gene regulatory regions that contain a binding site for the specified TF. Significant TFs are ranked according to importance (calculated as the product of TF occurrence and TF weight, as assigned by DiRE [Gotea and Ovcharenko, 2008]). In situ images from GenePaint.org (Set ID in brackets) of E14.5 intestinal cross sections for (**B**) RP58 (ZFP238) [MH813], (**C**) TAL1 [EH2794], (**D**) E47 (TCF3) [MH770], (**E**) NF1 [ES1724], (**F**) LDP1 (UBP1) [EN293], (**G**) ZID (ZBTB6) [MH3098], (**H**) ZIC3 [EB2075], (**I**) PAX4 [MH3124], (**J**) ROAZ (ZFP423) [MH1157], (**K**) JUN [MH524], (**L**) MEIS1 [EG1701], and (**M**) HOXA9 [EB2525].

et al., 2009; Liu et al., 2010; Tasian et al., 2010; Zacharias et al., 2011; Huang et al., 2013), and our studies here suggest that cJUN is a regulator of ME genes as well. However, we found no enrichment for predicted GLI TFBS within the cJUN peaks; only 54 predicted GLI TFBS were found within the 2741 cJUN peaks. Though it remains quite possible that these two regulatory factors bind separate enhancers for the same genes, it appears that the co-binding paradigm seen in the human cJUN promoter (Lanier-Plamberger et al., 2009; Amable et al., 2014) is not a prevalent regulatory pattern for ISM.

To further probe a possible regulatory relationship between cJUN and GLI in the control of ICM gene expression, we incubated E14.5 intestines in the presence or absence of the Hh inhibitor cyclopamine (Chen et al., 2002) and collected both of the transcriptome profiles using RNA-seq. We then examined the response of the verified ICM genes (Fig. 1AC). Of the 127 ICM

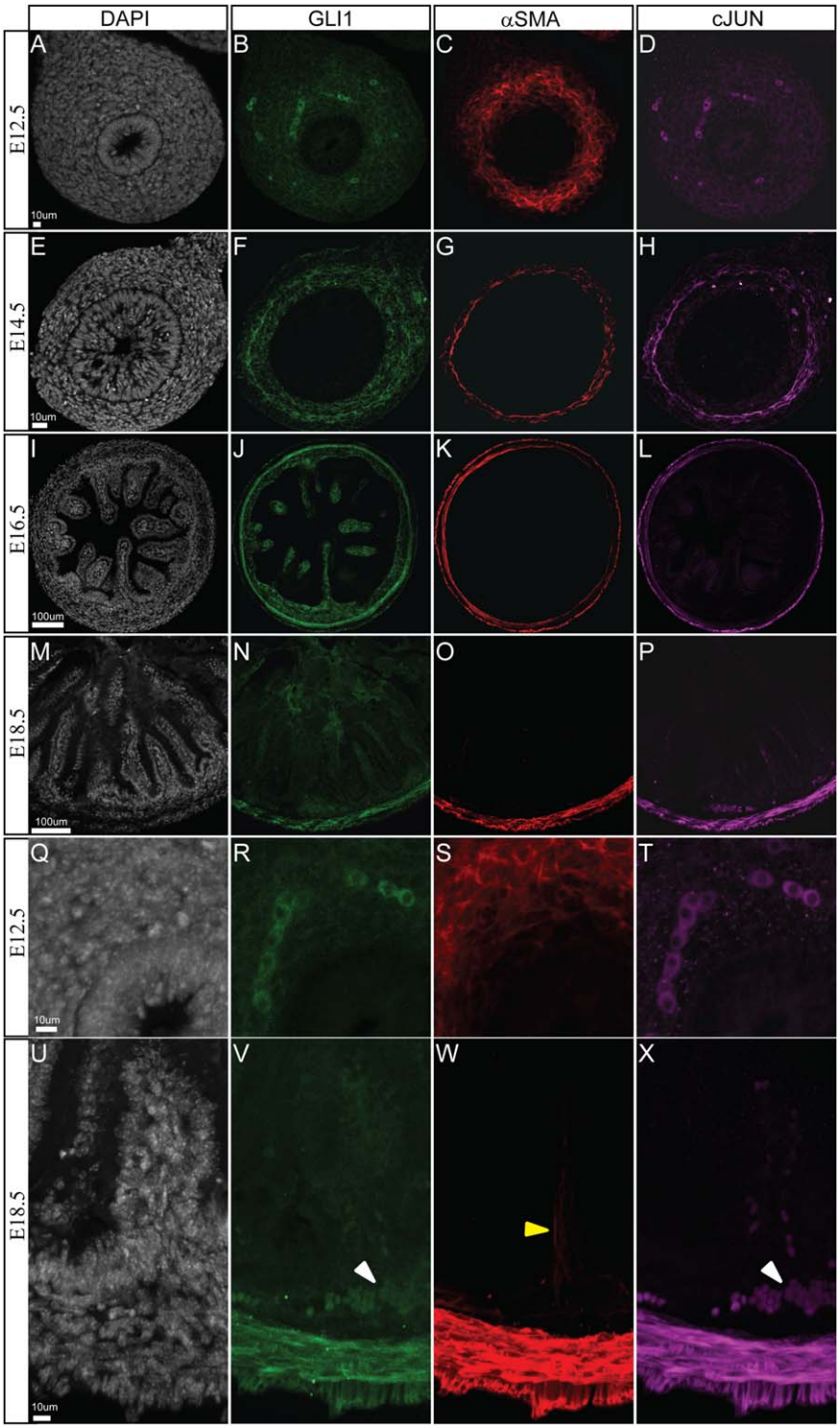

Fig. 3. GLI1 and cJUN co-localize with visceral smooth muscle during intestinal development. Intestines collected from *Gli1*$^{eGFP/+}$ mice were sectioned and stained for DAPI (gray), eGFP (green), the smooth muscle marker αSMA (red), and cJUN (purple) at E12.5 (**A–D; Q–T**), E14.5 (**E–H**), E16.5 (**I–L**) and E18.5 (**M–P; U–X**). cJUN co-localizes with αSMA in the inner circular muscles (ICM) and outer longitudinal muscles (OLM) within the GLI1 expression domain. GLI1 is also expressed in the mesenchymal cluster cells (J), where an essential role for Hedgehog (Hh) signaling has been demonstrated for villus development (Walton et al., 2012). At E18.5, GLI1 and cJUN stain an additional cell population (V,X; white arrowheads) within the mesenchyme. However, neither GLI1 nor cJUN co-localizes with villus smooth muscle (W; yellow arrowhead) at this time.

genes, 33% were down-regulated at least twofold by cyclopamine, confirming a substantial effect of Hh signaling on the maintenance of ICM gene expression. Among the other genes down-regulated by cyclopamine treatment were Hh pathway components (fold change adjusted P value < 0.05 [FC]: *Gli1*, -138.14; *Ptch2*, -51.27; *Hhip*, -29.86; *Ptch1*, -9.64; *Gli2*, -4.17)

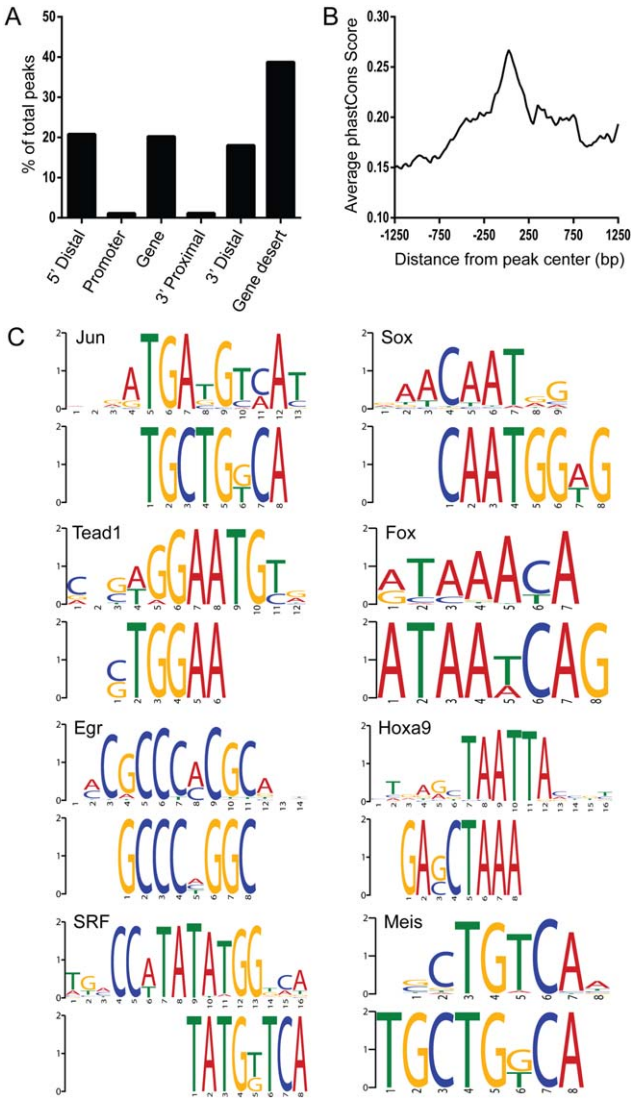

Fig. 4. Characterization of genomic regions bound by c-JUN in E14.5 intestine. **(A)** Distribution of peaks relative to the nearest transcription start site (TSS) or transcription end site (TES) of the closest gene. Location of the peak is categorized as within a gene if it is between the TSS and the TES; gene desert if it is > 100 Kbp from the gene; 5′ distal if it is between 100 Kbp and 2 Kbp upstream of the TSS; promoter if it is ≤ 2 Kbp upstream of the TSS; 3′ proximal if it is ≤ 2 Kbp downstream of the TES; or 3′ distal if it is between 2 Kbp and 100 Kbp from the TES. **(B)** Average vertebrate phastCons score for each nucleotide position mapped from the center of the peak. **(C)** Motif enrichment analysis (DREME) of the central 100 bps of the peaks identified several transcriptional factors involved in muscle development. Top-ranking motifs have the following corrected E values: Jun (4.20E-23), Sox (1.40E-43), Tead1 (1.10E-37), Fox (1.40E-29), Egr2 (5.00E-31), HoxA9 (1.40E-23), SRF (4.00E-14) and Meis (1.50E-12).

and other intestinal Hh target genes (FC: *Foxl1*, -31.56; *Foxf2*, -7.41; *Foxf1*, -3.84; *Grem1*, -3.56; *Myocd*, -2.13) (see Supp. Table S3, which is available online). Additional, down-regulated genes suggest similar roles for Hh in ISM to those previously seen in skeletal muscle (Duprez et al., 1998; Borycki et al., 1999; Pownall et al., 2002; Singh et al., 2012). These include modulators of Wnt signaling, genes affiliated with proliferation of muscle precursors, and genes involved in promotion of differentiation into muscle cells (Table 2).

Surprisingly, however, *cJun* itself was not strongly down-regulated by cyclopamine treatment (FC with adjusted P value > 0.05: -1.21), despite the fact that *cJun* is a Hh target in other settings (Kudo et al., 2012). To further investigate this finding, we used qPCR in C2C12 myoblast cells to test whether endogenous *cJun* responds to up-regulated Hh signaling induced by SAG treatment over an 8-hour period. These studies revealed that *cJun* transcription is up-regulated by increased Hh signaling with similar kinetics to PTCH1 up-regulation (Fig. 5B), consistent with the idea that *cJun* is a transcriptional target of Hh signaling in C2C12 cells. Additionally, we separated E14.5 intestinal mesenchyme from epithelium and cultured the isolated mesenchyme in the presence or absence of the Hh agonist SAG. Under these conditions, *cJun* was again up-regulated (FC: 2.30) at a comparable level to *Ptch1* (FC: 2.01) (Fig. 5C). Together, these data suggest that *cJun* is likely to be a direct Hh target in muscle cells, but that additional signals may maintain *cJun* levels (or the transcript may be very stable) in the context of the cyclopamine-treated whole intestine. In accord with the idea that acute reduction in Hh signaling by cyclopamine does not alter cJUN levels, only 7% of the genes associated with cJUN peaks (363/2741) were down-regulated by cyclopamine treatment.

Because *cJun* appears to be a direct target of Hh signaling in intestinal ISM, we looked for a Hh-responsive enhancer region that could be responsible for directing *cJun* transcription. In a previous study, we used kmer-SVM (Fletez-Brant et al., 2013), a machine learning method, to globally identify Hh regulatory regions (Submitted (Gurdziel et al., 2015)). That analysis identified a putative Hh enhancer upstream of *cJun* (chr4:94791492-94792702; build mm9). This genomic region was cloned into a luciferase reporter plasmid and co-transfected with a plasmid that drives constitutive expression of GLI1 in C2C12 cells (Vokes et al., 2007). As shown in Figure 6, this *cJun* enhancer is indeed activated by GLI1; this activation depends on the GLI1 binding site since expression of luciferase is attenuated when the enhancer GLI binding site is mutated (GKO, Fig. 6). These data establish a mechanism by which Hh signaling can activate cJUN in the ICM.

Conclusions

Using transcriptome profiling paired with in situ data sets, we have identified a catalog of 127 ISM genes with confirmed expression in the E14.5 ICM. Subsequent promoter analysis of co-clustered genes implicated cJUN as a regulatory component in ISM formation. Using ChIP-seq on intestinal tissue, we identified 2741 potential cJUN binding locations and found enrichment of other muscle TFBS within these regions, indicating that they are likely enhancers for visceral muscle genes. Previously, cJUN has been linked to proliferation of skeletal muscle and vascular smooth muscle (Kami et al., 1995) (Daury et al., 2001) (Yasumoto et al., 2001; Chiba et al., 2014); this study further enlarges this regulatory landscape to include ISM.

Since Hh is an important regulator of ISM gene expression, we further explored the possible regulatory relationships between cJUN and GLI in the regulation of ISM genes. Our data show that co-binding of the two transcription factors at the same enhancer is rare. However, *cJun* is likely a direct target of Hh signaling in the ICM (Fig. 5B,C), and we have identified an enhancer element in the *cJun* gene that could control this regulation. Thus, in addition to its direct effect on ISM gene transcription, Hh signaling could further influence ISM gene expression through induction

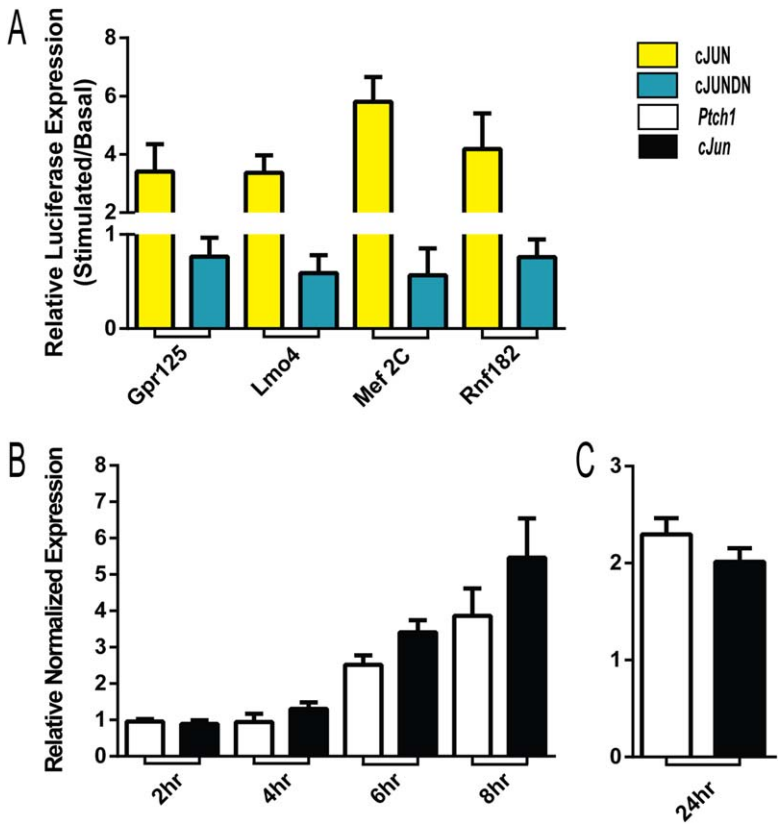

Fig. 5. Response of ISM enhancers to *cJun* and response of *cJun* to Hedgehog (Hh) signaling. **(A)** Putative regulatory regions from cJUN ChIP peaks, cloned upstream of a minimal luciferase promoter, were transfected into C2C12 cells with cJUN (yellow) or dominant negative cJUN (blue). Relative activity is plotted as stimulated (cJUN or cJUNDN)/basal. cJUN responsive enhancer activity was confirmed for regions annotated to *Gpr125*, *Lmo4*, *Mef2C* and *Rnf18*. In all cases, the comparisons for cJUN vs. cJUNDN were significant (unpaired t-test two-tailed P value < 0.01). **(B,C)** Relative transcript levels measured by qPCR. **(B)** Fold change of *Ptch1* (white) and *cJun* (black) comparing untreated and SAG-treated C2C12 cells at two-hour intervals after stimulation. **(C)** Fold change of *Ptch1* and *cJun* 24 hours after SAG treatment of E14.5 isolated mesenchyme tissue. Error bars (ABC) represent the standard deviation of three experimental replicates.

of *cJun*, which we establish as a regulator of ISM gene expression.

Experimental Procedures

Intestine Collection

Intestines were collected from C57BL/6J mouse fetuses at E14.5. Fetal stages were determined by date of coitus and confirmed by Theiler staging. Isolated intestines were grown on Transwell membranes with BGJb media supplemented with ascorbic acid (5mg/mL) and penicillin-streptomycin-glutamine (50mg/mL). Conditions were no treatment epithelial, no treatment mesenchyme, and whole intestines treated with cyclopamine (5 μM), as well as mesenchyme treated with or without SAG (1 μm) (Walton et al., 2012). After 24 hours of culture, the entire intestine from below the common bile duct to above the cecum was collected.

Epithelial-Mesenchymal Separation

Collected intestines were immersed in BD Biosciences Cell Recovery Solution for 1–2 hours at 4degC with gentle shaking. When the epithelial tissue began to separate from the mesenchyme tissue, forceps were used to mechanically separate the tissue into two distinct populations (Madison et al., 2005).

Immunohistochemistry

Intestines collected from *Gli1*$^{eGFP/+}$ mice at E12.5, E14.5, E16.5, and E18.5 were fixed overnight in 4% paraformaldehyde and then embedded in 7% agarose. Vibratome sections of 50 μm were permeabilized in 0.5% Triton X-100 for 25 minutes at room temperature and then blocked with 20% goat serum, 0.1% Tween 20 for 30 minutes. Sections were sequentially stained with rabbit anti-cJUN (1:400; Santa Cruz sc-44) overnight at 4degC followed by anti-rabbit secondary antibody for 45 minutes at room temperature (1:1000; Life Technologies A-21244), and then anti-GFP-488 (1:500; Life Technologies A-21311), anti-αSMA-CY3 (1:1000; Sigma C6198), and DAPI overnight at 4degC. Stained sections were mounted on slides with ProLong Gold and imaged on a Nikon A1 confocal microscope.

RNA Collection and mRNA-seq

Total RNA was collected for each sample using the Life Technologies mirVana™ miRNA Isolation Kit following the standard protocol. mRNA-seq on three biological replicates for each condition was performed by the University of Michigan DNA Sequencing Core following Illumina guidelines.

TABLE 2. Muscle Affiliated Genes Down-regulated by Attenuation of Hh Signaling

Gene	Fold change[a]	Affiliation	Reference
Dkk1	−84.45	Wnt modulator	He et al. 2013
Edar	−21.86	Wnt modulator	Wells et al. 2010
Sall1	−17.75	Wnt modulator	Kiefer et al. 2010
Mmp9	−16.22	Muscle stem cell	Zimowska et al. 2008
Epha8	−10.70	Muscle stem cell	Star et al. 2011
Il1b	−12.82	Muscle stem cell	Luo et al. 2003; Chen el al. 2006
Klhl14	−32.90	Muscle differentiation	Abou-Elhamd et al. 2009
Mir24-1	−8.34	Muscle differentiation	Sun et al. 2008

[a]Fold change is the gene expression level in the presence/absence of cyclopamine.

ChIP Assay

ChIP was performed following a previously described protocol (Vokes et al., 2007). Prior to experimental collection, antibodies (16 uL of 0.05 ug/uL into 100 uL) were coupled to magnetic beads (Dynabeads Protein G) at 4degC for 24 hours. Between six and eight pups harvested from the same litter were pooled for each ChIP experiment. Intestines were snap-frozen in liquid nitrogen and ground with a mortar and pestle to dissociate the tissue into single cells. DNA and protein were cross-linked with 1% formaldehyde for 10 minutes and then treated with 0.125 M glycine to halt the reaction. DNA was sonicated to an average fragment size of 500 bp. DNA fragments were incubated with cJUN (Polyclonal Rabbit; Santa Cruz sc-44 or sc-1694) or IgG (Polyclonal Rabbit; Santa Cruz sc-2027) bound beads overnight at 4degC. cJUN-bound DNA was eluted from the beads overnight at 70degC and purified with phenol-chloroform DNA extraction after RNase and DNase treatment. Both cJUN-immunoprecipitated and -input DNA were submitted to the University of Michigan DNA Sequencing Core for sequencing.

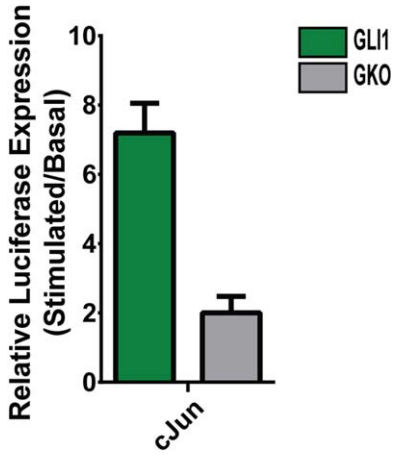

Fig. 6. Functional verification of GLI-dependent enhancer upstream of *cJun*. A putative Hedgehog (Hh) regulatory region upstream of *cJun* cloned upstream of a minimal luciferase promoter then co-transfected into C2C12 cells with a GLI1 expression vector exhibits characteristic Hh responsiveness (green). Specificity of the response is confirmed to be GLI dependent by mutagenesis of the GLI TFBS (GKO) (gray) (unpaired t-test two-tailed P value < 0.01). Error bars represent the standard deviation of three experimental replicates.

Sequencing and Data Analysis

RNA and DNA were sequenced on an Illumina HiSeq machine generating 50-cycle single reads. Reads containing up to one mismatch were mapped to the mouse reference genome (Build mm9) using Tophat for RNA (Trapnell et al., 2009) and Bowtie for DNA (Langmead et al., 2009). Three replicates were collected for each of the three conditions (isolated epithelium, isolated mesenchyme, and cyclopamine-treated whole intestine). Differential expression of RNA samples was determined using DESeq (Anders and Huber, 2010). ChIP peaks were identified using MACS (version 1.4) (Zhang et al., 2008). Raw and processed data files were deposited in GEO under accession number GSE74993.

qPCR

cDNA was reverse transcribed from 400 ug of RNA using the iScript kit. Three samples per condition were tested in triplicate with the following primer sets: (*18sRNA*: GTAACCCGTTGAACCCCATT, CCATCCAATCGGTAGTAGCG; *Rp113a*: GACC TCCTCCTTTCCCAGGC, GCCTCGGCCATCCAATACC; *Ptch1*: GGC TACTGGCCGGAAAGC, GAATGTAACAACCCAGTTTAAATAAGAGTCT; *cJun*: GTGTGGGACGACGATCAAAAG, TGACCAC TAACAGGGAAGGAC). After adjusting for primer efficiency (E), expression values for *cJun* (E: 107.1%) and *Ptch1* (E: 90.4%) were normalized to *18sRNA* (E: 98.4%) and *Rp113a* (E: 90.4%).

Computing Resources

Except where otherwise indicated, all computational steps were performed using custom Perl and R scripts.

Cluster Analysis

Hierarchical clustering analysis of transcript expression data was performed within Cluster 3.0 using uncentered correlation with average linkage (Eisen et al., 1998). Java TreeView was used to visualize the clustered data (Saldanha, 2004).

Conservation Analysis

A total of 1250 bp of sequence from both sides of the center of each peak was uploaded to the UCSC genome browser. The phastCons score (phastCons30way) for each nucleotide position was downloaded from the UCSC table browser. Scores were averaged across all peak positions and binned in 25-bp increments.

Motif Analysis

To identify enriched motifs, 100 bp of sequence from the center of each peak was submitted to DREME (Bailey, 2011). Discovered motifs were annotated using the JASPAR vertebrate database in Tomtom (Gupta et al., 2007).

Gene Set Enrichment Analysis

A gene list comprising the up-regulated mesenchyme genes was run using the GSEAPreranked tool (1000 permutations) (Subramanian et al., 2005).

Cloning of Putative Enhancer Regions

Putative enhancers were amplified from C57BL/6 genomic DNA (supplied by Jackson Laboratory) using template-specific PCR primers (*Gpr125*: GAGTGGAGTGGAAGGGGTTT, CTTTCTGCCAC TCCTTCTGC; *Lmo4*: GGAGAAGTACAACAGACCCTTCA, ACAATC ACAGCGAAGAAGCA; *Mef2C*: CCTAGCCAAAGTCATTGTGGA, GGCATCATCCTGAGTGAGGT; *Rnf182*: CCAGATTCAGTAGAGC ACCCA, TACCTACATGCGAAGGCAAG; *cJun*: CTTAAGTGTT-GAGGGCAGGCAG, CATGAGAAAATGCAGGGGATCT). A CACC extension was added to the end of one primer to facilitate directional cloning. PCR fragments were cloned into the pENTR/D--TOPO vector using the standard kit (Invitrogen) and then shuttled into the pGL3-promoter luciferase vector (Promega) using the Gateway cloning system (Invitrogen). QuikChange mutagenesis (Stratagene) was used to mutate putative GLI binding sites in the *cJun* regulatory region by replacing the C in the sixth position to a G (GAAAAGACAAGAGACCAGCCATCCCAGCCTTTGAT, ATC AAAGGCTGGGATGGCTGGTCTCTTGTCTTTTC; GAACTCCATGGG ACCAGCCAGAAGAGGCTGATG, CATCAGCCTCTTCTGGCTGG TCCCATGGAGTTC).

Luciferase Assay

C2C12 cells (35,000 per well) were plated on 12-well plates and grown with DMEM media supplemented with 10% fetal bovine serum, 1x penicillin, streptomycin and glutamate. After 24 hours, cells were Lipofectamine-transfected with 400 ng of the construct containing the putative enhancer region plus either a control vector, GLI1 (pCIG) (Vokes et al., 2007), cJUN (pMIEG3-c-Jun; Addgene 40348), or dominant negative cJUN (pMIEG3-JunDN; Addgene 40350) (in equal molecular weight). *Renilla* (Promega pRL-CMV) was also included to normalize transfection efficiency. After an additional 24 hours, cells were changed to serum-free media to promote ciliogenesis required for Hh signaling (Santos and Reiter, 2008). Cell lysates were collected after 48 hours and measured for luciferase activity using the Dual-Luciferase Reporter Assay System (Promega) on a PerkinElmer Wallac Victor3 1420 Multilabel Counter. Three experimental replicates were collected for each condition.

Acknowledgments

The authors would like to thank Dr. Will Zacharias for comments and Dr. Steve Vokes and Dr. Lihong Shi for generously providing advice on ChIP-seq. K.G. was supported by University of Michigan NIH Training Program in Basic and Translational Digestive Science T32 DK094775 and University of Michigan NIH Training Program in Bioinformatics T32 GM 70449Z. D.G. and K.W. both acknowledge support from National Institutes of Health P01 DK062041.

References

Abrams J, Davuluri G, Seiler C, Pack M. 2012. Smooth muscle caldesmon modulates peristalsis in the wild type and non-innervated zebrafish intestine. Neurogastroenterol Motil 24:288–299.

Alstead EM, Murphy MN, Flanagan AM, Bishop AE, Hodgson HJ. 1988. Familial autonomic visceral myopathy with degeneration of muscularis mucosae. J Clin Pathol 41:424–429.

Amable L, Gavin E, Kudo K, Meng E, Rocconi RP, Shevde LA, Reed E. 2014. GLI1 upregulates C-JUN through a specific 130-kDa isoform. Int J Oncol 44:655–661.

Anders S, Huber W. 2010. Differential expression analysis for sequence count data. Genome Biol 11:R106.

Antonucci A, Fronzoni L, Cogliandro L, Cogliandro RF, Caputo C, De Giorgio R, Pallotti F, Barbara G, Corinaldesi R, Stanghellini V. 2008. Chronic intestinal pseudo-obstruction. World J Gastroenterol 14:2953–2961.

Anuras S, Mitros FA, Nowak TV, Ionasescu VV, Gurll NJ, Christensen J, Green JB. 1983. A familial visceral myopathy with external ophthalmoplegia and autosomal recessive transmission. Gastroenterology 84:346–353.

Anuras S, Shaw A, Christensen J. 1981. The familial syndromes of intestinal pseudoobstruction. Am J Hum Genet 33:584–591.

Austin ED, Ma L, LeDuc C, Berman Rosenzweig E, Borczuk A, Phillips JA 3rd, Palomero T, Sumazin P, Kim HR, Talati MH, West J, Loyd JE, Chung WK. 2012. Whole exome sequencing to identify a novel gene (caveolin-1) associated with human pulmonary arterial hypertension. Circ Cardiovasc Genet 5:336–343.

Bailey TL. 2011. DREME: motif discovery in transcription factor ChIP-seq data. Bioinformatics 27:1653–1659.

Baker LA, Gomez RA. 1998. Embryonic development of the ureter and bladder: acquisition of smooth muscle. J Urol 160:545–550.

Benhaddou A, Keime C, Ye T, Morlon A, Michel I, Jost B, Mengus G, Davidson I. 2012. Transcription factor TEAD4 regulates expression of myogenin and the unfolded protein response genes during C2C12 cell differentiation. Cell Death Differ 19:220–231.

Berkes CA, Bergstrom DA, Penn BH, Seaver KJ, Knoepfler PS, Tapscott SJ. 2004. Pbx marks genes for activation by MyoD indicating a role for a homeodomain protein in establishing myogenic potential. Mol Cell 14:465–477.

Bitar KN. 2003. Function of gastrointestinal smooth muscle: from signaling to contractile proteins. Am J Med 115 Suppl 3A:15S–23S.

Borycki AG, Brunk B, Tajbakhsh S, Buckingham M, Chiang C, Emerson CP Jr. 1999. Sonic hedgehog controls epaxial muscle determination through Myf5 activation. Development 126:4053–4063.

Caubit X, Lye CM, Martin E, Core N, Long DA, Vola C, Jenkins D, Garratt AN, Skaer H, Woolf AS, Fasano L. 2008. Teashirt 3 is necessary for ureteral smooth muscle differentiation downstream of SHH and BMP4. Development 135:3301–3310.

Chen CN, Li YS, Yeh YT, Lee PL, Usami S, Chien S, Chiu JJ. 2006. Synergistic roles of platelet-derived growth factor-BB and interleukin-1beta in phenotypic modulation of human aortic smooth muscle cells. Proc Natl Acad Sci U S A 103:2665–2670.

Chen JK, Taipale J, Cooper MK, Beachy PA. 2002. Inhibition of Hedgehog signaling by direct binding of cyclopamine to Smoothened. Genes Dev 16:2743–2748.

Chi J, Rodriguez EH, Wang Z, Nuyten DS, Mukherjee S, Rijn M, Vijver MJ, Hastie T, Brown PO. 2007. Gene expression programs of human smooth muscle cells: tissue-specific differentiation and prognostic significance in breast cancers. PLoS Genet 3:1770–1784.

Chiba S, Sumi Y, Okayasu K, Okamoto T, Tateishi T, Furusawa H, Tsuchiya K, Fujie T, Tamaoka M, Sakashita H, Miyazaki Y, Inase N. 2014. The c-jun N-terminal kinase signaling pathway regulates airway smooth muscle cell proliferation. Eur Respir J 44.

Creemers EE, Sutherland LB, Oh J, Barbosa AC, Olson EN. 2006. Coactivation of MEF2 by the SAP domain proteins myocardin and MASTR. Mol Cell 23:83–96.

Daury L, Busson M, Tourkine N, Casas F, Cassar-Malek I, Wrutniak-Cabello C, Castellazzi M, Cabello G. 2001. Opposing functions of ATF2 and Fos-like transcription factors in c-Jun-

mediated myogenin expression and terminal differentiation of avian myoblasts. Oncogene 20:7998–8008.
Di Padova M, Caretti G, Zhao P, Hoffman EP, Sartorelli V. 2007. MyoD acetylation influences temporal patterns of skeletal muscle gene expression. J Biol Chem 282:37650–37659.
Diez-Roux G, Banfi S, Sultan M, Geffers L, Anand S, Rozado D, Magen A, Canidio E, Pagani M, Peluso I, Lin-Marq N, Koch M, Bilio M, Cantiello I, Verde R, De Masi C, Bianchi SA, Cicchini J, Perroud E, Mehmeti S, Dagand E, Schrinner S, Nurnberger A, Schmidt K, Metz K, Zwingmann C, Brieske N, Springer C, Hernandez AM, Herzog S, Grabbe F, Sieverding C, Fischer B, Schrader K, Brockmeyer M, Dettmer S, Helbig C, Alunni V, Battaini MA, Mura C, Henrichsen CN, Garcia-Lopez R, Echevarria D, Puelles E, Garcia-Calero E, Kruse S, Uhr M, Kauck C, Feng G, Milyaev N, Ong CK, Kumar L, Lam M, Semple CA, Gyenesei A, Mundlos S, Radelof U, Lehrach H, Sarmientos P, Reymond A, Davidson DR, Dolle P, Antonarakis SE, Yaspo ML, Martinez S, Baldock RA, Eichele G, Ballabio A. 2011. A high-resolution anatomical atlas of the transcriptome in the mouse embryo. PLoS Biol 9:e1000582.
DiSandro MJ, Li Y, Baskin LS, Hayward S, Cunha G. 1998. Mesenchymal-epithelial interactions in bladder smooth muscle development: epithelial specificity. J Urol 160:1040–1046.
Donnell AM, Doi T, Hollwarth M, Kalicinski P, Czauderna P, Puri P. 2008. Deficient alpha-smooth muscle actin as a cause of functional intestinal obstruction in childhood. Pediatr Surg Int 24: 1191–1195.
Duprez D, Fournier-Thibault C, Le Douarin N. 1998. Sonic Hedgehog induces proliferation of committed skeletal muscle cells in the chick limb. Development 125:495–505.
Eisen MB, Spellman PT, Brown PO, Botstein D. 1998. Cluster analysis and display of genome-wide expression patterns. Proc Natl Acad Sci U S A 95:14863–14868.
Ema M, Faloon P, Zhang WJ, Hirashima M, Reid T, Stanford WL, Orkin S, Choi K, Rossant J. 2003. Combinatorial effects of Flk1 and Tal1 on vascular and hematopoietic development in the mouse. Genes Dev 17:380–393.
Fan YY, Ye GH, Lin KZ, Yu LS, Wu SZ, Dong MW, Han JG, Feng XP, Li XB. 2013. Time-dependent expression and distribution of Egr-1 during skeletal muscle wound healing in rats. J Mol Histol 44:75–81.
Fletez-Brant C, Lee D, McCallion AS, Beer MA. 2013. kmer-SVM: a web server for identifying predictive regulatory sequence features in genomic data sets. Nucleic Acids Res 41:W544–556.
Gabella G. 1985. Structure of the musculature of the chicken small intestine. Anat Embryol (Berl) 171:139–149.
Giordano C, Powell H, Leopizzi M, De Curtis M, Travaglini C, Sebastiani M, Gallo P, Taylor RW, d'Amati G. 2009. Fatal congenital myopathy and gastrointestinal pseudo-obstruction due to POLG1 mutations. Neurology 72:1103–1105.
Gotea V, Ovcharenko I. 2008. DiRE: identifying distant regulatory elements of co-expressed genes. Nucleic Acids Res 36:1–7.
Goyal RK, Chaudhury A. 2008. Physiology of normal esophageal motility. J Clin Gastroenterol 42:610–619.
Gunning P, Ponte P, Kedes L, Eddy R, Shows T. 1984. Chromosomal location of the co-expressed human skeletal and cardiac actin genes. Proc Natl Acad Sci U S A 81:1813–1817.
Gupta S, Stamatoyannopoulos JA, Bailey TL, Noble WS. 2007. Quantifying similarity between motifs. Genome Biol 8:R24.
Gurdziel K, Vogt K, Schneider G, Richards N, Gumucio DL. 2015. Computational prediction and experimental validation of novel Hedgehog-responsive enhancers linked to genes of the Hedgehog pathway. BMC Development Biology. Available at: http://bmcdevbiol.biomedcentral.com.
Holla OL, Bock G, Busk OL, Isfoss BL. 2014. Familial visceral myopathy diagnosed by exome sequencing of a patient with chronic intestinal pseudo-obstruction. Endoscopy 46:533–537.
Huang H, Cotton JL, Wang Y, Rajurkar M, Zhu LJ, Lewis BC, Mao J. 2013. Specific Requirement of Gli Transcription Factors in Hedgehog-mediated Intestinal Development. J Biol Chem 288: 17589–17596.
Kami K, Noguchi K, Senba E. 1995. Localization of myogenin, c-fos, c-jun, and muscle-specific gene mRNAs in regenerating rat skeletal muscle. Cell Tissue Res 280:11–19.
Kedinger M, Simon-Assmann P, Bouziges F, Arnold C, Alexandre E, Haffen K. 1990. Smooth muscle actin expression during rat gut development and induction in fetal skin fibroblastic cells associated with intestinal embryonic epithelium. Differentiation 43:87–97.
Knoepfler PS, Bergstrom DA, Uetsuki T, Dac-Korytko I, Sun YH, Wright WE, Tapscott SJ, Kamps MP. 1999. A conserved motif N-terminal to the DNA-binding domains of myogenic bHLH transcription factors mediates cooperative DNA binding with pbx-Meis1/Prep1. Nucleic Acids Res 27:3752–3761.
Kolterud A, Grosse AS, Zacharias WJ, Walton KD, Kretovich KE, Madison BB, Waghray M, Ferris JE, Hu C, Merchant JL, Dlugosz AA, Kottmann AH, Gumucio DL. 2009. Paracrine Hedgehog signaling in stomach and intestine: new roles for hedgehog in gastrointestinal patterning. Gastroenterology 137:618–628.
Kossler N, Stricker S, Rodelsperger C, Robinson PN, Kim J, Dietrich C, Osswald M, Kuhnisch J, Stevenson DA, Braun T, Mundlos S, Kolanczyk M. 2011. Neurofibromin (Nf1) is required for skeletal muscle development. Hum Mol Genet 20:2697–2709.
Kudo K, Gavin E, Das S, Amable L, Shevde LA, Reed E. 2012. Inhibition of Gli1 results in altered c-Jun activation, inhibition of cisplatin-induced upregulation of ERCC1, XPD and XRCC1, and inhibition of platinum-DNA adduct repair. Oncogene 31:4718–4724.
Kumar CC, Mohan SR, Zavodny PJ, Narula SK, Leibowitz PJ. 1989. Characterization and differential expression of human vascular smooth muscle myosin light chain 2 isoform in nonmuscle cells. Biochemistry 28:4027–4035.
Laner-Plamberger S, Kaser A, Paulischta M, Hauser-Kronberger C, Eichberger T, Frischauf AM. 2009. Cooperation between GLI and JUN enhances transcription of JUN and selected GLI target genes. Oncogene 28:1639–1651.
Langmead, Trapnell C, Pop M, Salzberg SL. 2009. Ultrafast and memory-efficient alignment of short DNA sequences to the human genome. Genome Biol 10:R25.
Lee HJ, Goring W, Ochs M, Muhlfeld C, Steding G, Paprotta I, Engel W, Adham IM. 2004. Sox15 is required for skeletal muscle regeneration. Mol Cell Biol 24:8428–8436.
Lees-Miller JP, Heeley DH, Smillie LB, Kay CM. 1987. Isolation and characterization of an abundant and novel 22-kDa protein (SM22) from chicken gizzard smooth muscle. J Biol Chem 262: 2988–2993.
Lehtonen HJ, Sipponen T, Tojkander S, Karikoski R, Jarvinen H, Laing NG, Lappalainen P, Aaltonen LA, Tuupanen S. 2012. Segregation of a missense variant in enteric smooth muscle actin gamma-2 with autosomal dominant familial visceral myopathy. Gastroenterology 143:1482–1491.
Li L, Miano JM, Cserjesi P, Olson EN. 1996. SM22 alpha, a marker of adult smooth muscle, is expressed in multiple myogenic lineages during embryogenesis. Circ Res 78:188–195.
Liu B, Feng D, Lin G, Cao M, Kan YW, Cunha GR, Baskin LS. 2010. Signalling molecules involved in mouse bladder smooth muscle cellular differentiation. Int J Dev Biol 54:175–180.
Liu F, Wang X, Hu G, Wang Y, Zhou J. 2014. The transcription factor TEAD1 represses smooth muscle-specific gene expression by abolishing myocardin function. J Biol Chem 289:3308–3316.
Liu Z, Wang Z, Yanagisawa H, Olson EN. 2005. Phenotypic modulation of smooth muscle cells through interaction of Foxo4 and myocardin. Developmental Cell 9:261–270.
Madison BB, Braunstein K, Kuizon E, Portman K, Qiao XT, Gumucio DL. 2005. Epithelial hedgehog signals pattern the intestinal crypt-villus axis. Dev 132:279–289.
Meeson AP, Shi X, Alexander MS, Williams RS, Allen RE, Jiang N, Adham IM, Goetsch SC, Hammer RE, Garry DJ. 2007. Sox15 and Fhl3 transcriptionally coactivate Foxk1 and regulate myogenic progenitor cells. EMBO J 26:1902–1912.
Miano JM. 2003. Serum response factor: toggling between disparate programs of gene expression. J Mol Cell Cardiol 35:577–593.
Montalvo P, Paz L, Chiappa E, Aronne S, Novelli M, Biain ME. 2004. [Intestinal pseudo-obstruction due to sporadic visceral myopathy]. Medicina (B Aires) 64:525–528.
Mourikis P, Tajbakhsh S. 2014. Distinct contextual roles for Notch signalling in skeletal muscle stem cells. BMC Dev Biol 14:2.
Ohama T, Hori M, Momotani E, Iwakura Y, Guo F, Kishi H, Kobayashi S, Ozaki H. 2007. Intestinal inflammation

downregulates smooth muscle CPI-17 through induction of TNF-alpha and causes motility disorders. Am J Physiol Gastrointest Liver Physiol 292:G1429–1438.
Papanicolaou KN, Izumiya Y, Walsh K. 2008. Forkhead transcription factors and cardiovascular biology. Circ Res 102:16–31.
Pownall ME, Gustafsson MK, Emerson CP. 2002. Myogenic regulatory factors and the specification of muscle progenitors in vertebrate embryos. Annu Rev Cell Dev Biol 18:747–783.
Qiu H, Wang F, Liu C, Xu X, Liu B. 2011. TEAD1-dependent expression of the FoxO3a gene in mouse skeletal muscle. BMC Mol Biol 12:1.
Raines AM, Adam M, Magella B, Meyer SE, Grimes HL, Dey SK, Potter SS. 2013. Recombineering-based dissection of flanking and paralogous Hox gene functions in mouse reproductive tracts. Development 140:2942–2952.
Ramalho-Santos M, Melton DA, McMahon AP. 2000. Hedgehog signals regulate multiple aspects of gastrointestinal development. Development 127:2763–2772.
Saldanha AJ. 2004. Java Treeview—extensible visualization of microarray data. Bioinformatics 20:3246–3248.
Sanchez AM, Candau RB, Bernardi H. 2014. FoxO transcription factors: their roles in the maintenance of skeletal muscle homeostasis. Cell Mol Life Sci 71:1657–1671.
Santos N, Reiter JF. 2008. Building it up and taking it down: the regulation of vertebrate ciliogenesis. Dev Dyn 237:1972–1981.
Schmidt K, Glaser G, Wernig A, Wegner M, Rosorius O. 2003. Sox8 is a specific marker for muscle satellite cells and inhibits myogenesis. J Biol Chem 278:29769–29775.
Shiroyanagi Y, Liu B, Cao M, Agras K, Li J, Hsieh MH, Willingham EJ, Baskin LS. 2007. Urothelial sonic hedgehog signaling plays an important role in bladder smooth muscle formation. Differentiation 75:968–977.
Singh BN, Doyle MJ, Weaver CV, Koyano-Nakagawa N, Garry DJ. 2012. Hedgehog and Wnt coordinate signaling in myogenic progenitors and regulate limb regeneration. Dev Biol 371:23–34.
Sipponen T, Karikoski R, Nuutinen H, Markkola A, Kaitila I. 2009. Three-generation familial visceral myopathy with alpha-actin-positive inclusion bodies in intestinal smooth muscle. J Clin Gastroenterol 43:437–443.
Smith VV, Lake BD, Kamm MA, Nicholls RJ. 1992. Intestinal pseudo-obstruction with deficient smooth muscle alpha-actin. Histopathology 21:535–542.
Strasser P, Gimona M, Moessler H, Herzog M, Small JV. 1993. Mammalian calponin. Identification and expression of genetic variants. FEBS Lett 330:13–18.
Subramanian A, Tamayo P, Mootha VK, Mukherjee S, Ebert BL, Gillette MA, Paulovich A, Pomeroy SL, Golub TR, Lander ES, Mesirov JP. 2005. Gene set enrichment analysis: a knowledge-based approach for interpreting genome-wide expression profiles. Proc Natl Acad Sci U S A 102:15545–15550.
Sukegawa A, Narita T, Kameda T, Saitoh K, Nohno T, Iba H, Yasugi S, Fukuda K. 2000. The concentric structure of the developing gut is regulated by Sonic hedgehog derived from endodermal epithelium. Development 127:1971–1980.
Summers MA, Quinlan KG, Payne JM, Little DG, North KN, Schindeler A. 2015. Skeletal muscle and motor deficits in Neurofibromatosis Type 1. J Musculoskelet Neuronal Interact 15:161–170.
Tao T, Wasson J, Bernal-Mizrachi E, Behn PS, Chayen S, Duprat L, Meyer J, Glaser B, Permutt MA. 1998. Isolation and characterization of the human PAX4 gene. Diabetes 47:1650–1653.
Tasian G, Cunha G, Baskin L. 2010. Smooth muscle differentiation and patterning in the urinary bladder. Differentiation 80:106–117.
Teillet M, Watanabe Y, Jeffs P, Duprez D, Lapointe F, Le Douarin NM. 1998. Sonic hedgehog is required for survival of both myogenic and chondrogenic somitic lineages. Development 125: 2019–2030.
Thomason RT, Bader DM, Winters NI. 2012. Comprehensive timeline of mesodermal development in the quail small intestine. Dev Dyn 241:1678–1694.
Thorson W, Diaz-Horta O, Foster J, 2nd, Spiliopoulos M, Quintero R, Farooq A, Blanton S, Tekin M. 2014. De novo ACTG2 mutations cause congenital distended bladder, microcolon, and intestinal hypoperistalsis. Hum Genet 133:737–742.
Tollet J, Everett AW, Sparrow MP. 2001. Spatial and temporal distribution of nerves, ganglia, and smooth muscle during the early pseudoglandular stage of fetal mouse lung development. Dev Dyn 221:48–60.
Townsend PJ, Farza H, MacGeoch C, Spurr NK, Wade R, Gahlmann R, Yacoub MH, Barton PJ. 1994. Human cardiac troponin T: identification of fetal isoforms and assignment of the TNNT2 locus to chromosome 1q. Genomics 21:311–316.
Trapnell C, Pachter L, Salzberg SL. 2009. TopHat: discovering splice junctions with RNA-Seq. Bioinformatics 25:1105–1111.
van der Loop FT, Schaart G, Timmer ED, Ramaekers FC, van Eys GJ. 1996. Smoothelin, a novel cytoskeletal protein specific for smooth muscle cells. J Cell Biol 134:401–411.
Van der Vliet A, Tuinstra TJ, Rademaker B, Bast A. 1992. Role of the epithelium in the control of intestinal motility: implications for intestinal damage after anoxia and reoxygenation. Agents Actions 36:159–167.
Van Goethem G, Schwartz M, Lofgren A, Dermaut B, Van Broeckhoven C, Vissing J. 2003. Novel POLG mutations in progressive external ophthalmoplegia mimicking mitochondrial neurogastrointestinal encephalomyopathy. Eur J Hum Genet 11:547–549.
Vinkemeier U, Obermann W, Weber K, Furst DO. 1993. The globular head domain of titin extends into the center of the sarcomeric M band. cDNA cloning, epitope mapping and immunoelectron microscopy of two titin-associated proteins. J Cell Sci 106(pt 1): 319–330.
Visel A, Thaller C, Eichele G. 2004. GenePaint.org: an atlas of gene expression patterns in the mouse embryo. Nucleic Acids Res 32: D552–556.
Vissing J, Ravn K, Danielsen ER, Duno M, Wibrand F, Wevers RA, Schwartz M. 2002. Multiple mtDNA deletions with features of MNGIE. Neurology 59:926–929.
Vokes SA, Ji H, McCuine S, Tenzen T, Giles S, Zhong S, Longabaugh WJ, Davidson EH, Wong WH, McMahon AP. 2007. Genomic characterization of Gli-activator targets in sonic hedgehog-mediated neural patterning. Development 134:1977–1989.
Wada Y, Fujimori M, Suzuki J, Tsukioka K, Ito K, Sawa Y, Morishita R, Kaneda Y, Isobe M, Amano J. 2003. Egr-1 in vascular smooth muscle cell proliferation in response to allo-antigen. J Surg Res 115:294–302.
Walton KD, Kolterud A, Czerwinski MJ, Bell MJ, Prakash A, Kushwaha J, Grosse AS, Schnell S, Gumucio DL. 2012. Hedgehog-responsive mesenchymal clusters direct patterning and emergence of intestinal villi. Proc Natl Acad Sci U S A 109: 15817–15822.
Wang D, Chang PS, Wang Z, Sutherland L, Richardson JA, Small E, Krieg PA, Olson EN. 2001. Activation of cardiac gene expression by myocardin, a transcriptional cofactor for serum response factor. Cell 105:851–862.
Wang F, Wang H, Wu H, Qiu H, Zeng C, Sun L, Liu B. 2013. TEAD1 controls C2C12 cell proliferation and differentiation and regulates three novel target genes. Cell Signal 25:674–681.
Wang Z, Wang D, Hockemeyer D, McAnally J. 2004. Myocardin and ternary complex factors compete for SRF to control smooth muscle gene expression. Nature 428:185–189.
Wang Z, Wang Z, Wang D, Pipes G. 2003. Myocardin is a master regulator of smooth muscle gene expression. Proc Natl Acad Sci U S A 100:7129–7134.
Wangler MF, Gonzaga-Jauregui C, Gambin T, Penney S, Moss T, Chopra A, Probst FJ, Xia F, Yang Y, Werlin S, Eglite I, Kornejeva L, Bacino CA, Baldridge D, Neul J, Lehman EL, Larson A, Beuten J, Muzny DM, Jhangiani S, Gibbs RA, Lupski JR, Beaudet A. 2014. Heterozygous de novo and inherited mutations in the smooth muscle actin (ACTG2) gene underlie megacystis-microcolon-intestinal hypoperistalsis syndrome. PLoS Genet 10:e1004258.
Watanabe M, Layne MD, Hsieh C, Maemura K, Gray S, Lee M, Jain MK. 2002. Regulation of smooth muscle cell differentiation by AT-rich interaction domain transcription factors Mrf2alpha and Mrf2beta. Circ Res 91:382–389.
Whorwell PJ, McCallum M, Creed FH, Roberts CT. 1986. Non-colonic features of irritable bowel syndrome. Gut 27:37–40.

Yasumoto H, Kim S, Zhan Y, Miyazaki H, Hoshiga M, Kaneda Y, Morishita R, Iwao H. 2001. Dominant negative c-jun gene transfer inhibits vascular smooth muscle cell proliferation and neointimal hyperplasia in rats. Gene Ther 8:1682–1689.

Yokoyama S, Ito Y, Ueno-Kudoh H, Shimizu H, Uchibe K, Albini S, Mitsuoka K, Miyaki S, Kiso M, Nagai A, Hikata T, Osada T, Fukuda N, Yamashita S, Harada D, Mezzano V, Kasai M, Puri PL, Hayashizaki Y, Okado H, Hashimoto M, Asahara H. 2009. A systems approach reveals that the myogenesis genome network is regulated by the transcriptional repressor RP58. Dev Cell 17: 836–848.

Yu J, Carroll TJ, McMahon AP. 2002. Sonic hedgehog regulates proliferation and differentiation of mesenchymal cells in the mouse metanephric kidney. Development (Cambridge, England) 129:5301–5312.

Zacharias WJ, Madison BB, Kretovich KE, Walton KD, Richards N, Udager AM, Li X, Gumucio DL. 2011. Hedgehog signaling controls homeostasis of adult intestinal smooth muscle. Dev Biol 355:152–162.

Zhang Y, Liu T, Meyer CA, Eeckhoute J, Johnson DS, Bernstein BE, Nusbaum C, Myers RM, Brown M, Li W, Liu XS. 2008. Model-based analysis of ChIP-Seq (MACS). Genome Biol 9:R137.

Zhang ZG, Wall JR, Bernard NF. 1996. Tissue distribution and quantitation of a gene expressing a 64-kDa antigen associated with thyroid-associated ophthalmopathy. Clin Immunol Immunopathol 80:236–244.

DEVELOPMENTAL DYNAMICS